Thermal Overload Capability of Permanent Magnet Synchronous Motors Employing Scaling Laws

F. Pauli, A. Ruf, and K. Hameyer, *Senior Member, IEEE*

***Abstract*—This paper presents an approach to predict the thermal utilization of permanent magnet synchronous motors (PMSM), which geometrically varies, by employing scaling laws. Once a FE-simulation is performed for a reference machine analytical equations can be used to calculate magnetic quantities and losses of a machine with modified dimensions. These losses are used as an input for a scalable thermal model to determine the winding temperature of the machine. The thermal load is required to estimate the life time of the insulation system and the PMSM itself. The simplicity of the thermal model which is used here allows for short overall computing times. Both, radial and axial scaling are applied. In this paper downscaling is used to increase the thermal utilization of a PMSM.**

***Keywords*—Permanent magnet machines; Thermal stress**

I. Introduction

An increasing demand for electrical machines in traction applications leads to a great importance to manufacture machines with high power densities, using as few resources as possible. These machines are operated at a variety of different load points. High power outputs are usually needed in short time intervals of the various drive cycles of electric vehicles. Therefore the base power of the machine can be significantly smaller than the maximum output power. Scaling equations offer the possibility for a rapid adaptation of the machine for a specific application scenario. When it comes to the electromagnetic behavior of PMSMs, changing the machines' length is a widely used methodology. Stipetic, Zarko and Popescu offer a solution that also takes radial scaling in 2D simulations into account [2], [3] and [4]. In the aforementioned approach the cross section of the scaled machine is an exact image of the cross section of the reference machine. By changing the current density reciprocal to the radius, also the magnetic fields inside the core of the scaled model, can be kept exact images of the fields inside the reference machine. Additionally to scaling electromagnetic properties of PMSMs,in this paper also mechanical and thermal issues are considered. This can be done by using a thermal model. In this paper a low order thermal model similar to the suggested models in [6] or [8] is used, which allows for short computation times. To parametrize the model measuring data is used. In [9], [10] and [11] advanced studies on the thermal properties of electrical machines are carried out, which allow for a more precise prediction of the thermal behavior. Linking the electromagnetic and thermal model offers a concept to predict the utilization of a scaled machine. The model also offers the possibility to apply driving-cycles or similar concepts to estimate the winding temperature and the lifetime of the machine depending on its size and application.

F. Pauli and K. Hameyer are with the Institute of Electrical Machines of RWTH Aachen University, Schinkelstr. 4, 52062 Aachen (e-mail: florian.pauli@iem.rwth-aachen.de).

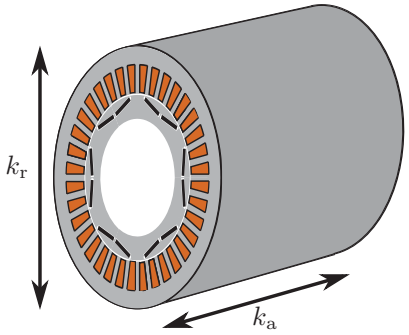

Fig. 1. Scaling of a PMSM.

II. Electromagnetic Scaling

The scaling equations for current density J, current I, flux linkage Ψ, torque T, ohmic resistance R, copper- and iron losses P_{Cu} and P_{Fe} are given in equations (1) - (7). k_a and k_r are the factors for axial and radial scaling (see Fig. 1). For some quantities the end-winding and the core area have to be considered separately. They are marked with the index ew (end-winding) respectively co (core). Scaled quantities are marked with the prime symbol. The scaling laws are taken from [2].

Based on the Maxwell equations, it can be shown that by applying eq. (1) the field distributions in the modified and reference machine are identical. The current can be calculated by integrating along the conductor cross sectional area. As the current density decreases by $\frac{1}{k_r}$ and the cross section increases by k_r^2 the current is given in eq. (2). The scaling factor for the flux linkage is calculated in a similar way: The flux density is unaffected while the coil surface in the core area increases by $k_a k_r$ and in the end-winding area by k_r^2. This results in eq. (3). Equations (4) - (7) can be derived from the basic mathematical description of PMSMs.

$$J' = \frac{1}{k_\mathrm{r}} \cdot J \tag{1}$$

$$I' = k_\mathrm{r} \cdot I \tag{2}$$

$$\Psi' = k_\mathrm{a} k_\mathrm{r} \Psi_\mathrm{co} + k_r^2 \Psi_\mathrm{ew} \tag{3}$$

$$T' = k_\mathrm{r}^2 k_\mathrm{a} T \tag{4}$$

$$R' = R'_\mathrm{co} + R'_\mathrm{ew} = \frac{k_\mathrm{a}}{k_\mathrm{r}^2} R_\mathrm{co} + \frac{1}{k_\mathrm{r}} R_\mathrm{ew} \tag{5}$$

$$P'_{Cu} = k_\mathrm{a} \cdot P_\mathrm{Cu,co} + k_\mathrm{r} \cdot P_\mathrm{Cu,ew} \tag{6}$$

$$P'_{Fe} = k_\mathrm{a} \cdot k_\mathrm{r}^2 \cdot P_\mathrm{Fe} \tag{7}$$

The equations above can be applied on quantities that are evaluated in d-q-component-current-maps for constant speed. Maximum input voltage and current of an electrical machine

978-1-5386-2476-0/18/$31.00 ©2018 IEEE

are often limited by the converter or the insulation system of the PMSM. In this paper the limits are unchanged.

Applying this assumption, a methodology for scaling quantities directly within the torque-speed map is presented. Such maps are often used to show load-point dependent loss-components or efficiencies. Recalculating the voltage cannot be performed using one simple scaling factor. As shown in equation (8) the flux linkage and the voltage drop due to ohmic losses have different factors. Also flux linkage and resistance that derive from the end-winding are distinguished from the quantities that derive from the core.

$$\begin{aligned}\mathbf{V}'_{\mathrm{dq}} &= (\frac{k_\mathrm{a}}{k_\mathrm{r}} R_{co} + R_{\mathrm{ew}}) \cdot \mathbf{I}'_{\mathrm{dq}} + \frac{d}{dt}(k_\mathrm{a} k_\mathrm{r} \mathbf{\Psi}_{\mathrm{ew,co}} + k_r \mathbf{\Psi}_{\mathrm{dq,ew}}) \\ &+ \begin{pmatrix} 0 & \omega_{el} \\ -\omega_{\mathrm{el}} & 0 \end{pmatrix} (k_\mathrm{a} k_\mathrm{r} \mathbf{\Psi}_{\mathrm{dq,co}} + k_r \mathbf{\Psi}_{\mathrm{dq,ew}}) \end{aligned} \quad (8)$$

If the axial length of the machine is not significantly smaller than its radius, the flux linkage of the end-winding is comparatively small. Except for low speeds the ohmic losses only add little to the overall voltage drop. Thus eq. (8) can be simplified:

$$\begin{aligned}\mathbf{V}'_{\mathrm{dq}} &= k_\mathrm{a} k_\mathrm{r} (\frac{d}{dt} \mathbf{\Psi_{dq,co}} + \begin{pmatrix} 0 & \omega_{el} \\ -\omega_{el} & 0 \end{pmatrix} \mathbf{\Psi_{dq,co}}) \\ &= k_\mathrm{a} k_\mathrm{r} \mathbf{V}_{\mathrm{dq}} \end{aligned} \quad (9)$$

In this paper a combination of the maximum torque per ampere (MTPA) and maximal torque per flux (MTPF) current control strategy is used. Thus the d- and q-components of the current are chosen to control a certain torque such that the overall current becomes minimal. At higher speed the maximum voltage of the machine has to be considered and an additional field weakening current has to be applied. Using

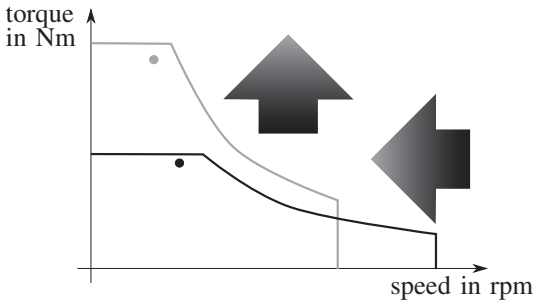

Fig. 2. Effect of scaling with $k_\mathrm{r} > 1$ on the operation range.

the simplified equation a direct scaling of the torque-speed map can be performed, assuming that the maximum output voltage of the converter is constant. The map is stretched by $k_a k_r^2$ along the torque axis and by $1/(k_a k_r)$ along the speed axis (see Fig. 2). The copper losses can be scaled as shown in (6). In equations (1) - (7) the speed is assumed to be constant. However, as shown in the IEM-5-parameter-formula to calculate iron losses which is introduced in [7] the iron losses are frequency-dependent:

$$\begin{aligned} P_{Fe} &= a_1 \hat{B}^2 f + a_2 \hat{B}^2 f^2 (1 + a_3 \hat{B}^{a_4}) + a_5 \hat{B}^{1.5} f^{1.5} \\ &= P_{\mathrm{hyst}} + P_{\mathrm{class}} + P_{\mathrm{sat}} + P_{\mathrm{exc}} \end{aligned} \quad (10)$$

Considering eq. (7), the frequency dependency of the loss components in eq. (10) and the stretching of the speed axis, the scaling equation of the iron losses can be expressed by:

$$\begin{aligned} P'_{Fe}(n') &= k_\mathrm{r}^2 k_\mathrm{a} P_{Fe}(n') \\ &= k_\mathrm{r}^2 k_\mathrm{a} \left[\frac{1}{k_\mathrm{r} k_\mathrm{a}} P_{\mathrm{hyst}}(n) + \frac{1}{k_\mathrm{r}^2 k_\mathrm{a}^2} (P_{\mathrm{class}}(n) + P_{\mathrm{sat}}(n)) \right. \\ &\qquad \left. + \frac{1}{k_\mathrm{r}^{1.5} k_\mathrm{a}^{1.5}} P_{exc}(n) \right] \\ &= k_\mathrm{r} P_{\mathrm{hyst}}(n) + \frac{1}{k_\mathrm{a}} (P_{\mathrm{class}}(n) + P_{\mathrm{sat}}(n)) \\ &\qquad + \sqrt{\frac{k_\mathrm{r}}{k_\mathrm{a}}} P_{exc}(n) \end{aligned} \quad (11)$$

It can be seen that the iron losses for a certain load point become smaller when downscaling the PMSM even though the fluxdensity in the stator iron increases. This behavior can be explained by the reduced core volume.

III. SCALING OF THE MAXIMUM SPEED

The rotation of the machine causes centrifugal forces and mechanical stress on the rotor. As shown in Fig. 3 the highest force density can be found inside the bridges. At a constant

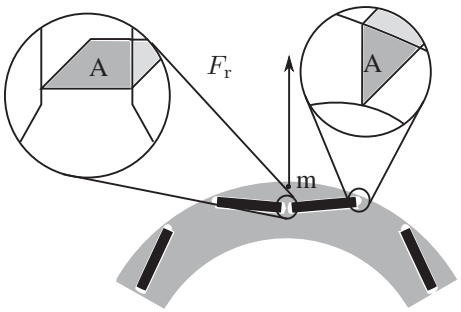

Fig. 3. Centrifugal force inside the rotor.

speed the mechanical stress inside the rotor varies when the radius is changing. The force on a point mass m which is rotating with a speed n, at a radius of r and the mechanical stress σ on a surface segment dA are given by eq. (12) and (13):

$$F = 4\pi^2 m r n^2 \quad (12)$$

$$\sigma = \frac{dF}{dA} \quad (13)$$

The mass is proportional to the volume and increases with $k_r^2 k_a$, the radius is proportional with k_r and the surface segment with $k_r k_a$. Thus a constant stress can be achieved by scaling the speed with $1/k_r$.

$$\sigma' = \frac{d(4\pi m' r' n'^2)}{dA'} = \frac{d(4\pi k_r^2 m k_r r \frac{n^2}{k_r^2})}{k_r dA} = \sigma \quad (14)$$

As the maximum stress occurs at the highest speed, the speed limit also decreases with $1/k_r$. It should be noted that the axial scaling factor of the machine cannot be chosen arbitrarily as the stiffness of the shaft limits the maximum motor length.

IV. THERMAL SCALING

The thermal behavior of any object is determined by its thermal capacitances and heat transfer. The capacitance C is given by eq. (15) where c is the specific capacitance and V is the object's Volume.

$$C = c \cdot V \tag{15}$$

There are three known mechanisms of heat transfer: thermal conduction, convection and radiation. The heat transfer due to thermal conduction $\dot{Q}_\lambda$ through an object with a constant cross section A can be expressed by equation (16). d is the length of the object, λ is the thermal conductivity and ΔT is the difference of the temperature. The convective heat transfer $\dot{Q}_\lambda$ occurs on an object's surface and depends on ΔT and the convective coefficient α. The thermal energy which is exchanged between two objects with temperatures T_1 and T_2 due to radiation is expressed by eq. (18). σ is the Stefan Boltzmann constant and ϵ the emissivity.

$$\dot{Q}_\lambda = \lambda \frac{A}{d} \Delta T \tag{16}$$

$$\dot{Q}_\alpha = \alpha A \Delta T \tag{17}$$

$$\dot{Q}_\epsilon = \sigma \epsilon A (T_1^4 - T_2^4) \tag{18}$$

All these quantities depend on physical dimensions which are directly depending on k_a an k_r. Heat transfer and thermal capacitances can be expressed as functions of the scaling factors. The machine which is regarded in this paper is cooled by an active rotor cooling and a water jacket cooling. Here it is assumed that the entire rotor losses are dissipated through the shaft. The stator losses are assumed to be completely dissipated by the water jacket cooling. Thus rotor and stator are decoupled. Focusing on the winding temperature, the thermal behavior can be described using a low-order model. For the studied machine the topology in Fig. 4 is proposed. Fig. 5 presents in which way the thermal resistances and capacitances are assigned to the stator. The copper- respectively iron losses are imposed to the corresponding nodes.

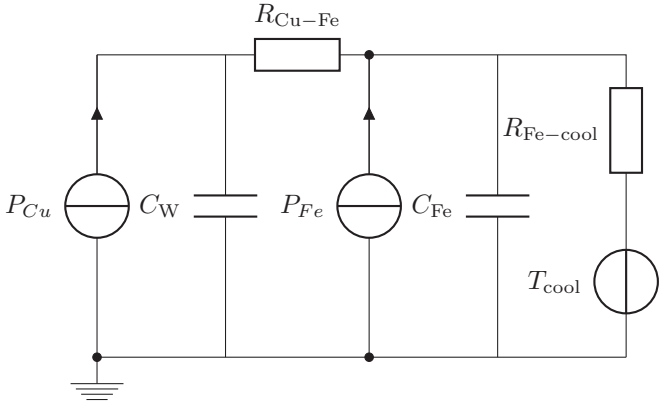

Fig. 4. Second order thermal model of a PMSM.

C_{Fe} is the thermal capacitance of the stator core. It changes with the same factor as the volume when the machine is scaled:

$$C'_{Fe} = k_{\mathrm{a}} k_r^2 C_{Fe} \tag{19}$$

Regarding the thermal capacitance of the winding C_W, the conductors inside the stator slots and in the end-winding have to be distinguished as the end-winding is not effected by the axial scaling:

$$C'_W = k_a k_r^2 C_{W,co} + k_r^3 C_{W,ew} \tag{20}$$

In this model only radial heat flow is regarded. In the real machine the losses from the end-winding are conducted into the stator slots. As the thermal resistance of copper is small when compared to the resistance of the remaining heat path, here it is assumed that the entire copper losses are generated in the slots. The thermal resistance due to conduction is given by eq. (21) resulting in the scaling equation for the thermal resistance R_{Cu-Fe} eq. (22).

$$R_\lambda = \frac{1}{\lambda} \cdot \int_{x_1}^{x_2} \frac{dx}{A(x)} \tag{21}$$

$$R'_{Cu-Fe} = \frac{1}{k_{\mathrm{a}}} R_{Cu-Fe} \tag{22}$$

The heatflow between stator core and water jacket cooling is dominated by convection. Such a resistance only depends on the convection coefficient α and the surface area A (see eq. (23)).Thus $R_{Fe-cool}$ is given by eq. (24).

$$R_\alpha = \frac{1}{\alpha A} \tag{23}$$

$$R'_{Fe-cool} = \frac{1}{k_{\mathrm{r}} k_{\mathrm{a}}} R_{\mathrm{Fe-cool}} \tag{24}$$

Using the equations for electromagnetic scaling, the losses for an operating point in the torque-speed map can be calculated. Applying the scaled thermal model of the PMSM, the end-winding temperatures for different operating scenarios can be estimated. Using lifetime estimating such as proposed in [1], the results can be used to estimate the time to failure of the winding system. The approach of adapting a thermal network when the machine is scaled can be used for any thermal network. However, for more detailed networks the parameters might not be directly linked to the machine dimensions. The diameter of the enameled wires in the winding for example are often fixed to a certain value. Approaches of modeling this region can be taken from [9], [10] and [11].

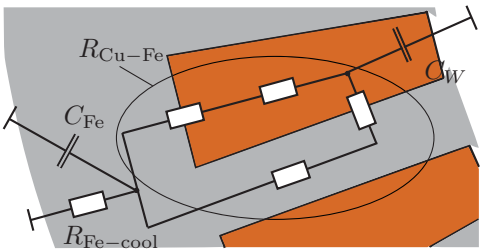

Fig. 5. Assignment of resistances and capacitances of the thermal model to the stator geometry.

V. APPLICATION

The scaling laws are applied to a PMSM, which is designed for a traction application in electric vehicles. An overview of the PMSM's parameters is given in tab. I.

TABLE I. QUANTITIES OF THE UNSCALED PMSM

quantity	symbol	value
rated Power	P_N	$22\ kW$
rated Torque	T_N	$70\ Nm$
maximum speed	n_max	$10000\ rpm$
number of pole pairs	p	3
number of phases	m	3
number of turns	N	8
number of slots	N_slot	36
radius of the stator	r_stat	$101\ mm$
length of the core	l_core	$80\ mm$

In order to identify the values of thermal capacitances and resistances the winding temperature is measured for a variety of load points. A pattern-search algorithm is used to identify the parameters. It is required to define start values and limits for each parameter. The start values for the capacitances are calculated using the volumes and material properties of the stator iron and winding. The volumes of iron, copper and insulation material are listed below:

- $V_\mathrm{Fe} = 1033\ cm^3$
- $V_\mathrm{Cu} = 587\ cm^3$
- $V_\mathrm{insulation} = 747\ cm^3$

The material properties are given in tab. II. As not all details about the insulation system are known, density and specific heat capacity are estimated using typical values for epoxy. The start values for the thermal resistances are based on

TABLE II. MATERIAL PROPERTIES

Material	density	specific heat capacity
Iron	$7600\ kg/m^3$	$450\ J/(kgK)$
copper	$8920\ kg/m^3$	$382\ J/(kgK)$
insulation	$1100\ kg/m^3$	$1400\ J/(kgK)$
aluminium	$2710\ kg/m^3$	$896\ J/(kgK)$

measurements. For a no-load operating point the copper losses become zero, as long as no field weakening current is applied. The measured loss power is equal to the iron loss power P_Fe. The only path the heat flow can take is through $R_\mathrm{Fe-cool}$. Therefore, in steady state, the thermal resistance is given by eq. (25). $P_\mathrm{Fe,stator}$ are the stator iron losses. The ratio of stator iron losses to entire iron losses is taken from an electromagnetic FE-simulation and equals 0.85 for the regarded operating point. It is used to calculate the stator iron losses from the overall iron losses, which are taken from the measuring data.

$$R_\mathrm{Fe-cool} = \frac{T_\mathrm{Cu} - T_\mathrm{cool}}{P_\mathrm{Fe,stator}} \tag{25}$$

The temperature of the coolant, the winding and the corresponding losses at this point are listed below:

- $T_\mathrm{cool} = 80°C$
- $T_\mathrm{Cu} = 85.2°C$
- $P_\mathrm{Fe,stator} = 607\ W$

The start values, and identified parameters for the thermal model are given in tab. III. For the thermal capacitance of the stator, the capacitances of the stator lamination and the housing are summed. A magnetic FE-simulation is performed

TABLE III. PARAMETERS OF THE THERMAL MODEL

parameter	start value	identified value
C_W	$3152\ J/K$	$4685\ J/K$
C_Fe	$6838\ J/K$	$10242\ J/K$
$R_\mathrm{Fe-cool}$	$0.0086\ K/W$	$0.0100\ K/W$
$R_\mathrm{Cu-Fe}$	$0.0257\ K/W$	$0.0338\ K/W$

to calculate the torque-speed map of the reference machine. In order to apply the aforementioned methodology for scaling the PMSM the following components of the total loss power have to be separated: copper losses of the winding head and the conductors inside the stator slots and the different components of the iron losses according to eq. (10). In Fig. 6 (a) the overall losses of the reference and of that one which is radially scaled by a factor of $k_r = 0.9$ are compared. For low speeds and high torques the losses of the downscaled machine are higher than for the reference machine as more current is needed for the same torque. It can be seen that the maximum speed of the scaled machine is higher than the maximum speed of the reference machine.

In Fig. 6 (b) the reference machine and an axially scaled PMSM with $k_a = 0.9$ are compared. In this case the losses for small speeds and high torques are also increased but not as much as for the radially scaled machine.

Applying the scaling equations on the thermal model yields the values which are given in tab. IV. The losses

TABLE IV. PARAMETERS OF THE SCALED THERMAL MODELS

param	ref.	rad. scal	ax. scal
C_W	$4685\ J/K$	$3547\ J/K$	$4379\ J/K$
C_{Fe}	$10242\ J/K$	$9217\ J/K$	$8296\ J/K$
$R_{Fe-cool}$	$0.0100\ K/W$	$0.0111\ K/W$	$0.0111\ K/W$
R_{Cu-Fe}	$0.0257\ K/W$	$0.0257\ K/W$	$0.0285\ K/W$

from the FE-simulation are used to calculate the thermal behavior at a given load-point. A point at $4000\ rpm$ and $52.5\ Nm$ is chosen. In Fig. 7 the winding temperature is shown for all three PMSMs. At the chosen point the overall losses for scaled and reference machines are roughly the same. However, due to the higher copper losses and the thermal resistances of the scaled machines the end-winding temperature increases. The temperature of the PMSM with a smaller radius rises the fastest and is the highest in steady state. The fast increase of the temperature can be accounted to the low thermal capacitances. In the following the maximum winding temperature is defined to be $180\ °C$. The operating range of the scaled machines and the reference machine is investigated. This can be performed by evaluating each point on the torque-speed map using the thermal model. This procedure yields the operation ranges displayed in Fig. 8. For low speed the continous operation torque (S1) of the scaled machines is decreased as the thermal resistances and copper losses increase. In field weakening operation the iron losses of the scaled machines are smaller. Thus for high speeds the higher thermal resistances are compensated and the S1-operating range is limited by about the same torque for all investigated machines. For the intermediate operation

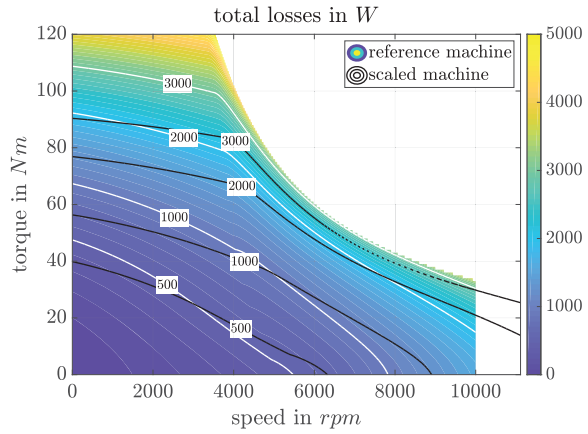

(a) Reference machine compared to a radially scaled machine with $k_r = 0.9$.

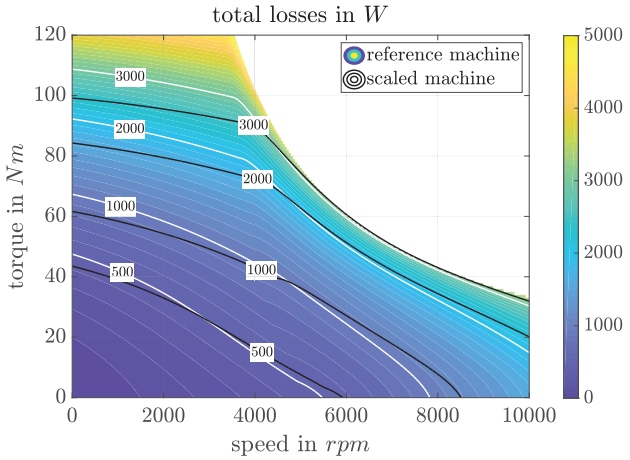

(b) Reference machine compared to an axially scaled machine with $k_a = 0.9$.

Fig. 6. Total losses of the reference machine compared to scaled machines.

(S2), also the thermal capacitances have an influence on the operating range. They are decreased by downscaling. Thus, also the maximum torque is decreased more significantly.

A machine that is operated as a traction drive faces a great number of different load points in the torque speed map. In this paper we study a transporter for an urban area. Its properties are given in table V. Applying driving-cycles only

TABLE V. PROPERTIES OF THE VEHICLE

quantity	symbol	value
total mass	m	1550 kg
drag coefficient	C_{w}	0.4
reference surface	A_{ref}	3.6 m^2

a discrete amount of load points for a deterministic operating scenario can be investigated. Thus, in this paper a statistical distribution of load points is applied to investigate the thermal utilization of the PMSM. The distribution represents the changing load points during operation that occur due to the traffic or road conditions that make it impossible to keep exactly the same speed for a longer time.

Averaging the acceleration of a vehicle within a certain speed

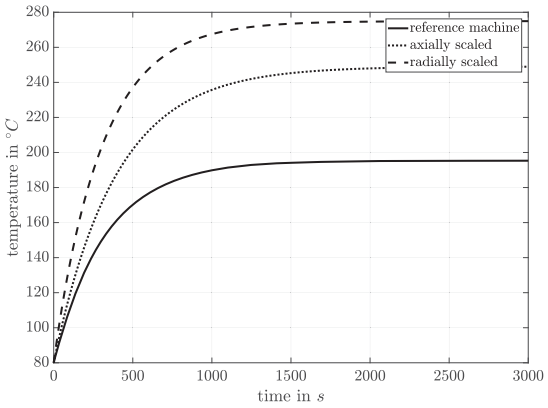

Fig. 7. Thermal respond to a load-point at 4000 rpm and 52.5 Nm.

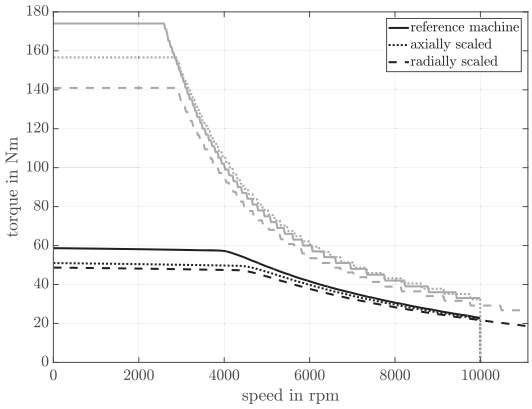

(a) Operating range for S1-operation.

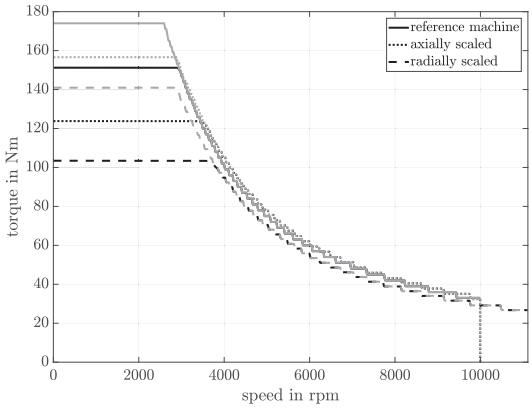

(b) Operating range for S2-operation.

Fig. 8. Thermal limits of the operating range for S1- and S2-operation.

range always yields zero. Thus the corresponding average torque is just high enough to cover all friction losses. In Fig. 9 (a) this average torque is displayed for a slope of 0 % and a slope of 10 %. It can be seen that the torque to overcome the steepness of the slope is significantly higher than the torque, which is needed to cover the losses. The load points are distributed around the average torque and are limited by the machine's maximum and minimum torque. In Fig. 9 (b) this

distribution is shown for the Worldwide Harmonized Light-Duty Vehicles Test Cycle (WLTC) Class two is shown for a vehicle that is operated on a $0\ \%$-slope. The torque-speed map is divided into a number of equally sized intervals along the speed axis and the standard deviations of the torque within each interval are displayed.
The beta-distribution is a probability distribution that is defined on a closed interval $[a, b]$ by eq. (26).

$$f(x) = \frac{1}{B(a,b,p,q)}(x-a)^{p-1}(b-x)^{q-1}$$
$$where\ B(a,b,p,q) = \int_a^b (u-a)^{p-1}(b-u)^{q-1}du \quad (26)$$

The operating range of the PMSM represents this interval when the distribution is used to model the machine being operated as a traction drive. The paramters p and q can be used to set the expected value and the standard deviation of the distribution. Using this approach, the thermal utilization of the PMSMs in two scenarios is studied: an operation close to the maximum speed of 85.2 (maximum speed of the WLTC class 2) for a long period of time on a flat ground and an operation at about 50 km/h on a 10-$\%$-slope for a short period of time. The first scenario represents a long drive on the highway. For this purpose a beta-distributed set of load points from the interval with the highest speed is taken and the corresponding losses are used as inputs for the thermal model. In Fig. 10 (a) the winding temperature for such an operation is plotted. It can be seen that the temperature of the radially scaled machine is significantly higher than for the other machines. Also the temperature curve is not that smooth as its time constant is smaller than for the other PMSMs. The second scenario represents an uphill-drive. Here a certain torque is needed to overcome the gravitation, thus the mean torque is taken from the dashed curve in Fig. 9 (a). The transporter can only be operated in such an scenario for a limited time span. As it is shown in Fig. 10 (b) in steady state especially the winding-temperature of the radially scaled machine exceeds the temperature index of the winding insulation (about $180°C$) by far. However, a short operation in this scenario for about $5\ min$ is possible without overheating the winding. As such an operation is only performed for a limited amount of time (by nature the length of a the slope the vehicle is operated on is limited), the machine matches the requirements of the studied vehicle.
An increased temperature leads to a shorter lifespan. The halving index in $°C$ (HIC) of modern insulation systems is $8...10\ °C$. The temperature index (TI) is about $180...190\ °C$. Thus the lifetime of the reference machine and the axially scaled machine is much higher than needed for the investigated application purpose. The radially scaled machine is operated at temperatures that match its temperature index. Thus the expected lifetime for modern insulation systems is about $20000\ h$. This exceeds the expected lifespan of the whole vehicle. Regarding this aspect the radially scaled machine would be the most sustainable as it needs the least amount of resources to be manufactured. In table VI the losses of the machines when they are operated in each of the two scenarios for ten minutes are presented. As the losses of the axially scaled machine are the smallest it might be the most economical solution. Also less resources for manufacturing are needed than for the reference machine.

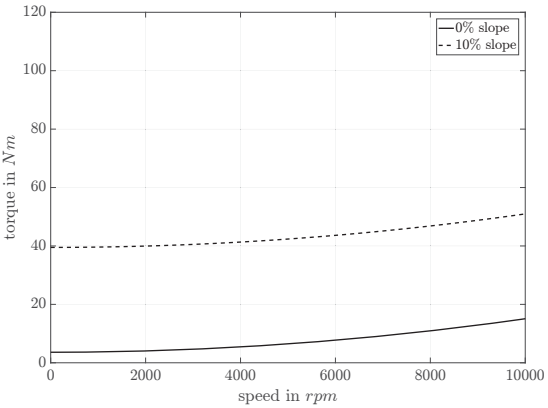

(a) Torque for a constant speed.

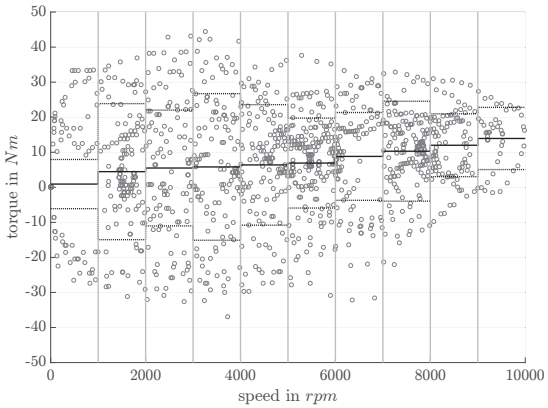

(b) Operating points of the WLTC in different speed intervals.

Fig. 9. Different representations of the WLTC.

TABLE VI. LOSSES FOR 10 MINUTES OF OPERATION

PMSM	scenario 1	scenario 2
reference machine	$0.344\ kWh$	$0.237\ kWh$
axially scaled	$0.306\ kWh$	$0.236\ kWh$
radially scaled	$0.351\ kWh$	$0.298\ kWh$

VI. CONCLUSION

The scaling equations of [2] are extended by an approach that allows for a direct scaling of losses and efficiency in the torque-speed map. The equations are applied to an exemplary PMSM. Using the results on a scalable thermal model the influence of the machine size on the thermal behavior can be studied. As expected it is shown that the thermal utilization for a downscaled machine is higher in most applications. Using an example of a transporter, the overload capability of scaled and reference machine is investigated using statistical distributions. Allowing for overload during the design process of a PMSM can lead to smaller machines, that use less resources and still match the specifications. As shown for the axially scaled machine, a smaller machine can also be more efficient for a specific application purpose. Thus the design

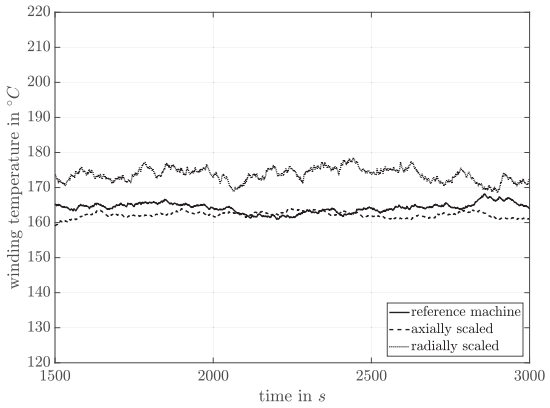

(a) Winding temperature in steady state at 85.2 km/h.

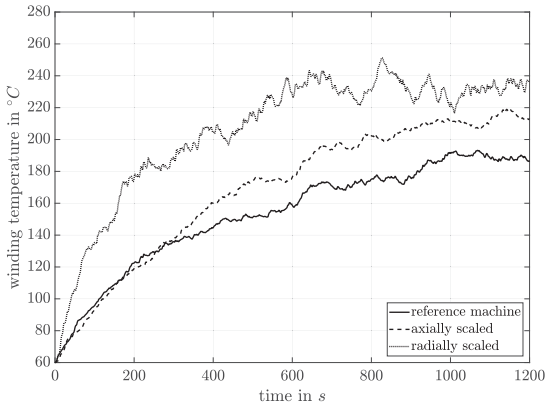

(b) Winding temperature at a 10 % slope and a speed of 50 km/h.

Fig. 10. Winding temperatures for different application scenarios.

process requires sufficient information about the application purpose of the machine: operating a vehicle on a slope utilizes the traction machine significantly more than on a flat ground. All methods that are introduced are based on analytical equations. Thus the adaptation of a machine for a certain operating scenarion can be performed rapidly.

REFERENCES

[1] R. Rothe, K. Hameyer, "Life Expectancy Calculation for Electric Vehicle Traction Motors Regarding Dynamic Temperature and Driving Cycles," International Electric Machines and Drives Conference, IEMDC, Rom, 2011

[2] S. Stipetic, D. Zarko and M. Popescu, "Scaling laws for synchronous permanent magnet machines," Ecological Vehicles and Renewable Energies (EVER), 2015 Tenth International Conference on, Monte Carlo, 2015, pp. 1-7.

[3] S. Stipetic, J. Goss: "Calculation of efficiency maps using scalable saturated flux linkage and loss model of a synchronous motor," 2016 XXII International Conference on Ecological Vehicles and Renewable Energies (EVER), 2016, pp. 1380-1386

[4] S. Stipetic, D. Zarko, M. Popescu: "Ultra-fast axial and radial scaling of synchronous permanent magnet machines," IET Electrical Power Applications 10 ,2016, pp. 658-666

[5] R. W. Wood, "Scaling Magnetic Systems", IEEE TRANSACTIONS ON MAGNETICS, VOL. 47, NO. 10, OCTOBER 2011

[6] T. Huber, W. Peters and J. Böcker, "A low-order thermal model for monitoring critical temperatures in permanent magnet synchronous motors," 7th IET International Conference on Power Electronics, Machines and Drives (PEMD 2014), Manchester, 2014, pp. 1-6.

[7] S. Steentjes, M. Lemann and K. Hameyer, "Advanced iron-loss calculation as a basis for efficiency improvement of electrical machines in automotive application", International Conference on Electrical Systems for Aircraft, Railway and Ship Propulsion (ESARS), Bologna, 2012

[8] A. Boglietti, M. Cossale, S. Vaschetto and T. Dutra, "Winding Thermal Model for Short-Time Transient: Experimental Validation in Operative Conditions," in IEEE Transactions on Industry Applications, vol. 54, no. 2, pp. 1312-1319, March-April 2018.

[9] N. Simpson, R. Wrobel and P. H. Mellor, "Estimation of Equivalent Thermal Parameters of Impregnated Electrical Windings," in IEEE Transactions on Industry Applications, vol. 49, no. 6, pp. 2505-2515, Nov.-Dec. 2013.

[10] R. Wrobel, S. Ayat and J. Godbehere, "A systematic experimental approach in deriving stator-winding heat transfer," 2017 IEEE International Electric Machines and Drives Conference (IEMDC), Miami, FL, 2017, pp. 1-8.

[11] J. L. Baker, R. Wrobel, D. Drury and P. H. Mellor, "A methodology for predicting the thermal behaviour of modular-wound electrical machines," 2014 IEEE Energy Conversion Congress and Exposition (ECCE), Pittsburgh, PA, 2014, pp. 5176-5183.

Florian Pauli received the M.Sc. degree in electrical engineering from RWTH Aachen University, Germany, in April 2017. He has been working as a research associate at the Institute of Electrical Machines since May 2017. His research interests include iron loss computations, thermal behavior, overload capability, lifetime models and the characterization of Insulation Systems of electrical machines.

Andreas Ruf received the M.Sc. degree in electrical engineering from Ruhr University Bochum (RUB), Germany, in August 2012. He has been working as a research associate at the Institute of Electrical Machines since January 2013. His research interests include iron loss computations, thermal behavior, overload capability, lifetime models, the design and control of electrical machines.

Kay Hameyer (IEEE M96 - SM99) Received 1986 the M.Sc. degree in electrical engineering from the University of Hannover, Germany, 1992 his Ph.D. degree from University of Technology Berlin, Germany for working on permanent magnet excited machines. After his university studies he worked with the Robert Bosch GmbH in Stuttgart, Germany, as a design engineer for permanent magnet servo motors. From 1988 to 1993 he was a member of staff at the University of Technology Berlin, Germany.

From 1996 to 2004, he was then a Full Professor of Numerical Field Computations and Electrical Machines, Katholieke Universiteit Leuven (KU Leuven), Leuven, Belgium. Since 2004, he has been a Full Professor and the Director of the Institute of Electrical Machines (IEM), RWTH Aachen University, Aachen, Germany.

His research interest focuses on all aspects of the design, control and manufacturing of electrical machines and the associated numerical simulation. The characterization and modeling of hard- and soft-magnetic materials is another focus of his work.

He has authored/coauthored more than 250 journal publications, more than 500 international conference publications and four books. His research interests include numerical field computation and optimization, the design and control of electrical machines, in particular, permanent-magnet excited machines, induction machines.

Dr. Hameyer is a member of the German VDE, a senior member of IEEE and a Fellow of the Institution of Engineering and Technology, U.K.